Video Article

Multiplexed Immunofluorescence Analysis and Quantification of Intratumoral PD-1$^+$ Tim-3$^+$ CD8$^+$ T Cells

Clémence Granier[1], Emeline Vinatier[2,3,4], Elia Colin[2,3], Marion Mandavit[2,3], Charles Dariane[2,3,5], Virginie Verkarre[6], Lucie Biard[7], Rami El Zein[2], Corinne Lesaffre[2], Isabelle Galy-Fauroux[2], Hélène Roussel[2,3,6], Eléonore De Guillebon[8], Charlotte Blanc[2,3], Antonin Saldmann[4], Cécile Badoual[2,6], Alain Gey*[4], Éric Tartour*[2,4]

[1]PARCC-INSERM U970, Université Paris Descartes

[2]INSERM U970, Université Paris Descartes

[3]Equipe Labellisée Ligue Contre le Cancer

[4]Department of Immunology, Hopital Européen Georges Pompidou

[5]Department of Medical Urology, Hopital Européen Georges Pompidou

[6]Department of Pathology, Hopital Européen Georges Pompidou

[7]Université Paris Diderot Paris 7

[8]Department of medical oncology, Hopital Européen Georges Pompidou

*These authors contributed equally

Correspondence to: Clémence Granier at clemence.granier@aphp.fr, Éric Tartour at eric.tartour@aphp.fr

URL: https://www.jove.com/video/56606
DOI: doi:10.3791/56606

Keywords: Cancer Research, Issue 132, Multiplex *in situ*, multispectral imaging, immunofluorescence technique, digital imaging, renal cell carcinoma, Tim-3, PD-1, tumor microenvironment, checkpoint inhibitors, *in situ* single cell analysis

Date Published: 2/8/2018

Citation: Granier, C., Vinatier, E., Colin, E., Mandavit, M., Dariane, C., Verkarre, V., Biard, L., El Zein, R., Lesaffre, C., Galy-Fauroux, I., Roussel, H., De Guillebon, E., Blanc, C., Saldmann, A., Badoual, C., Gey, A., Tartour, É. Multiplexed Immunofluorescence Analysis and Quantification of Intratumoral PD-1$^+$ Tim-3$^+$ CD8$^+$ T Cells. *J. Vis. Exp.* (132), e56606, doi:10.3791/56606 (2018).

Abstract

Immune cells are important components of the tumor microenvironment and influence tumor growth and evolution at all stages of carcinogenesis. Notably, it is now well established that the immune infiltrate in human tumors can correlate with prognosis and response to therapy. The analysis of the immune infiltrate in the tumor microenvironment has become a major challenge for the classification of patients and the response to treatment.

The co-expression of inhibitory receptors such as Program Cell Death Protein 1 (PD1; also known as CD279), Cytotoxic T Lymphocyte Associated Protein 4 (CTLA-4), T-Cell Immunoglobulin and Mucin Containing Protein-3 (Tim-3; also known as CD366), and Lymphocyte Activation Gene 3 (Lag-3; also known as CD223), is a hallmark of T cell exhaustion. We developed a multiparametric *in situ* immunofluorescence staining to identify and quantify at the cellular level the co-expression of these inhibitory receptors. On a retrospective series of frozen tissue of renal cell carcinomas (RCC), using a fluorescence multispectral imaging technology coupled with an image analysis software, it was found that co-expression of PD-1 and Tim-3 on tumor infiltrating CD8$^+$ T cells is correlated with a poor prognosis in RCC. To our knowledge, this represents the first study demonstrating that this automated multiplex *in situ* technology may have some clinical relevance.

Video Link

The video component of this article can be found at https://www.jove.com/video/56606/

Introduction

In the past few years, immunotherapy has emerged as a very promising treatment for many types of cancers, including RCC. Particularly, immunotherapy based on the inhibition of inhibitory checkpoints like PD-1 and CTLA-4 has been reported to be clinically effective[1,2,3,4,5,6]. Monoclonal antibodies against CTLA-4, PD-1, or Program Death Ligand 1 (PD-L1) are already approved in several cancers and lead to long lasting clinical responses in more than 20% of patients[7]. Nevertheless, not all patients are responders, the cost of the treatment is high, and these treatments are toxic, leading to potential serious autoimmune-like side effects. Therefore, the current challenge is to identify predictive markers to those new immunotherapies. The rate of mutations in the tumor, the expression of PD-L1, or the levels of intratumoral CD8$^+$ T cell infiltration have been reported to correlate with clinical response. However, this association is still too weak to recommend the use of these clinical biomarkers in clinical practice except for the companion test for PD-L1 before the administration of Pembrolizumab in non-small cell lung cancer (NSCLC) patients[8,9,1011,12]. It has been demonstrated that the co-expression of many inhibitory receptors like PD-1, Tim-3, Lag-3, and CTLA-4, induces a cell exhaustion phenotype and resistance to therapy[13,14,15]. Since peripheral blood is not representative of the tumor microenvironment, it is of high interest to analyze the phenotypic features of the cells *in situ*. PD-1 and Tim-3 co-expressing T cells are known to

be functionally impaired cells in several contexts[13,16,17]. In this study, the prognostic impact of the co-expression of the two inhibitory receptors PD-1 and Tim-3 on $CD8^+$ T cells was assessed.

Up until now, studying the co-expression of multiple markers on tumor infiltrating lymphocytes (TILs) has mainly been performed by flow cytometry analysis, making it necessary to work on fresh tumors and therefore precluding retrospective analyses. With conventional *in situ* staining, only one staining at a time can be performed, and the characterization of the cell type that co-expresses the markers is not possible. For example, PD-L1 is expressed by many cell types of the tumoral microenvironment, making it difficult to define by conventional immunohistochemistry analysis which cells expressing PD-L1 are the more relevant for correlative studies. In this work, we developed an innovative *in situ* multiparametric immunofluorescence method with computer-counting to correlate the co-expression of PD-1 and Tim-3 by tumor infiltrating $CD8^+$ T-cells with clinical outcomes in RCC. This technique has several advantages, including the possibility to analyze at a single cell level and multiple markers at the same time using a multispectral camera that can capture restricted intervals >10 nm through liquid crystal filters[18]. Moreover, the procedure is automatic which enables an inter-operator reproducibility and a shortened analysis compared to manual techniques[19]. In the cancer field, several studies reported convincing multiple stainings of immune molecules like PD-1, PD-L1, and CD8 in Merkel-cell carcinoma, lung cancer, and head and neck cancer[20,21,22,23]. The automated cell count is possible with training by the user (phenotyping step). The fluorescence is measured in the different cell compartments (nuclei, cytoplasm, and membrane).

Here, different subsets of tumor-infiltrating $CD8^+$ T cells expressing PD-1 and/or Tim-3 in a large cohort of RCC were counted and the results were correlated with clinical gravity scores and survival parameters. It was also possible to analyze membrane fluorescence intensity at the cellular resolution with Mean Fluorescence Intensity (MFI) data like in cytometry. As far as we know, this represents the first study reporting prognostic results using this multispectral imaging based count technique.

Protocol

This study was conducted in accordance with the Declaration of Helsinki and was approved by the local ethics committee (CPP Ile de France nr. 2012-05-04). Informed consent was obtained from the participant included in the cohorts.

1. Tissue Material

1. Collect RCC tissue samples on the day of surgery. Handle the surgical specimen at room temperature (pathology department).
2. Collect a tumor sample of approximately 0.5 cm x 0.5 cm x 0.5 cm size in a dry tube. Snap freeze in liquid nitrogen and store at -80 °C.
3. Coat the samples in optimal cutting temperature compound. Section the samples with a cryostat at -20 °C into 4 - 6 µm thick sections. Let the samples air dry on slides for 12 h and directly store them at -80 °C to avoid desiccation.
4. Check the quality of the sample by viewing a Hematoxylin and Eosin stained section.

2. *In Situ* Immunofluorescence Staining of TILs

1. **Procedural guidelines**
    1. Perform all experimental steps at room temperature.
    2. For all steps, perform the dilutions with Tris Buffer Saline (TBS; see **Table of Materials**).
    3. Perform the wash in TBS for all the steps except after the primary antibody incubation. For the latter, use Tris Buffer Saline Tween20 (TBST, see **Table of Materials**). For buffer composition and reconstitution see **Supplemental Table 1**.
    4. Use a humidity chamber for antibody incubations and a staining jar for washing.
    5. Do not let the section dry out during the procedure.

2. **Pretreatment**
    1. Thaw the slide containing the tissue sample and carefully dry the slide around the specimen with a paper towel. Delimitate the reaction area containing the tissue with a hydrophobic barrier pen (see **Table of Materials**). Dry for 2 min.
    2. Fix the samples in 100% acetone for 5 min, dry for 2 min, and wash with TBS for 10 min.

3. **Saturation and blockade**
    1. Pretreat the slides for 10 min with 3 drops of avidin 0.1%, tap and/or flick the slide to distribute the avidin and remove air bubbles, and then treat for 10 min with 3 drops of biotin 0.01% (see **Table of Materials**), tap, and/or flick. Wash with TBS.
    2. Perform an Fc receptors blockade. Apply 100 µL of a 5% volume/volume of normal serum diluted in TBS. Use serum from the same host species as the labeled secondary or tertiary antibody (see **Table of Materials**); here, donkey serum was used. Incubate for 30 min.
    3. During the incubation, briefly spin the anti-CD8, PD-1, and Tim-3 antibodies (**Table of Materials**). Prepare the mix of primary antibodies in TBS as described in **Supplemental Table 2**.

4. **Immuno-staining for CD8, PD-1, and Tim-3**
    1. Prepare the primary antibody mixture. Refer to **Table of Materials** and **Supplemental Table 2** for the antibodies used (anti-CD8, PD-1, Tim-3, and their corresponding secondary antibodies) and their concentrations.
    2. Tap and/or flick the remaining donkey serum (added in step 2.3.2). Incubate the slides with 100 µL of the non-labeled primary antibodies mix for 1 h in a humidified chamber.
    3. During the incubation, briefly spin the Cyanine 5 anti-rabbit, AF488-anti-goat, and biotinylated anti-mouse antibodies, and prepare the mix of secondary antibodies as described in **Supplemental Table 2**.
    4. Wash the slides in TBST for 5 min. Dry the slides.
    5. Incubate the slides with 100 µL of the secondary antibodies for 30 min in a humidified chamber.
    6. Prepare the mixture of tertiary antibody containing Cy3-streptavidin as described in **Supplemental Table 2**.

7. Wash the slides in TBS for 10 min. Dry the slides.
8. Incubate the slides with 100 µL of the tertiary antibody mixture for 30 min.
9. Wash the slides in TBS for 10 min. Dry the slides.

5. **Cell mounting**
   1. Mount the slides in a 4',6-Diamidino-2-Phenylindole, Dihydrochloride (DAPI)-containing mounting medium (1.5 µg/mL DAPI) with a coverslip compatible for fluorescence microscopy (see **Table of Materials**).
      NOTE: As a negative control for each experiment, one slide with isotype-matched antibodies was used at the same concentration as corresponding antibodies. For this staining, we used mouse IgG1, rabbit IgG, and goat IgG negative control antibodies (see **Table of Materials**). As a positive control, we used human hyperplasic tonsil which is known to be positive for the tested markers, for each experiment. A typical staining is described in the results (**Figure 1**). Mono-staining of CD8, PD-1, and Tim-3 should be performed individually (one staining per slide) with the same pre-treatment and without DAPI. A slide in the same experimental conditions without any antibody and only DAPI mounting medium should also be performed. A slide should be imaged using identical experimental conditions without any antibody and without DAPI.

3. Fluorescence Analysis and Automated Cell Count

1. **Image acquisition with the automated microscope**
   1. Create a protocol.
      1. Turn on the automated microscope software and the fluorescence illuminator.
      2. In the menu bar, click on "File," "create protocol," select "DAPI," "FITC," and "TRITC."
      3. Click "Next," "Tissue section," and click "Next," "Protocol name." Choose a name, for example, "CD8-PD-1-Tim-3," click "Next," and "save."
      4. Manually place a slide on the stage.
      5. In the menu bar, click "setup," "settings." Click "set home Z" in the new window.
      6. Adjust exposure time with a positive control slide *i.e.* a CD8, PD-1 and Tim-3 triple-stained with DAPI sample.
      7. In the control bar click “set exposure.”
      8. Adjust the exposure time for each filter until a sufficient but not saturating signal is obtained.
      9. For monochrome imaging, perform the following:
      10. Select acquisition and under 'autofocus' choose DAPI filter.
      11. In the "scan area limit", move the objective upper to the upper left corner of the slide. Click "Mark". Do the same for the lower right corner.
          NOTE: This step delimitates the area of low power imaging (LP imaging) at 4X; be aware to place the mark well so as to surround all the samples of the series.
      12. For high power (HP) imaging, perform the following:
      13. Under 'Autofocus', choose "DAPI".
      14. Under 'Acquisition' band, choose "DAPI", "FITC", "Cy3", and "Cy5". Click "OK". On the menu bar click "File", "Save protocol".
   2. Scan the slides.
      1. Load the protocol by clicking "File", "load protocol" from the menu bar. Click "Start".
      2. Enter 'Lab ID' (folder location for image storage). Enter Slide ID to identify the slide. Click "Next".
      3. Click "Monochrome Imaging" (to scan the whole slide under bright field light and acquire sequential images using a 4x objective).
         NOTE: This produces a grayscale overview of the slide.
      4. Click "Find Specimen". Select the area of tissue to be scanned at low resolution (4x): hold the 'Ctrl' key and click on a field using the cursor to select or deselect fields (**Figure 2A**).
      5. Click "LP Imaging" (4x imaging) for fluorescent Red Blue Green image acquisition of each field.
      6. For HP field selection, hold down 'Ctrl' key and click on a field using the cursor to select or deselect fields that correspond to the area of tissues that will be scanned at high resolution (20x). Select 5 fields (**Figure 2B**).
      7. Click "HP Imaging" (20x imaging) for a multispectral image acquisition of each field (**Figure 2C**).
      8. Click "Data Storage" to store images in the folder that was selected at the beginning in LabID.
         NOTE: The process is summarized and illustrated in **Figure 2**. For each step (tissue detection, field selection) an algorithm can be incremented and trained by the user for a whole-automated scan process.

2. **Fluorescence image analysis and automated cell counting with coupled analysis software**
   1. Build the spectral library.
      1. Open the image analysis software.
      2. On the left panel, open "Build libraries". Under 'load image', click on "Browse" and select one mono-stained image (*e.g.*, CD8/ Cyanine 5).
      3. Select the fluorophore, (*e.g.*, Cyanine 5). Click "extract". Click "Save" to store in library. Click "Save".
      4. Repeat the same process for PD-1, Tim-3, and DAPI mono-stained slides in order to integrate the spectrum of each fluorophore of interest.
         NOTE: Building the spectral library integrates the spectrum for each fluorophore used for the specific tissue (here, kidney), but "synthetic" libraries that already exist can be used. As the autofluorescence spectrum is strictly relative to the tissue, it is important to perform one auto-fluorescence and spectral library per project.
   2. Create a new project.
      1. From the menu bar, click "File", "New Project". In the 'Find feature' tab, select "cell segmentation". In the 'Phenotyping' tab, select "phenotyping". Click "Create".

2. Integrate the representative images in the project.
    1. In the 'File' tab, click on "open image". Choose 10 to 30 representative images of the whole series. Add the non-stained slide to remove autofluorescence. On the right panel: select library source. Select fluorophore and choose those corresponding to the spectral library previously built.

3. To remove tissue autofluorescence, click the "AF button" and then select the area of autofluorescence on the blank slide.
4. Image treatment and composite image generation.
    1. Click "Prepare all" to integrate the fluorescence library and the autofluorescence spectra to generate the composite image (**Figure 3**). Click on the 'eye' icon to open the 'view editor' panel and select the data displayed: select the markers CD8, PD-1, Tim-3, and DAPI. Remove the autofluorescence. Follow the steps presented by the software.

5. Segment the cells.
    1. To segment the cells, in 'Compartment', select "Nuclei" and "Membrane". In the "Nuclei" tab, set DAPI as the nuclear counterstain.
    2. In the 'Maximum and Minimum Size (px)' tab enter "40" and "176" as minimum and maximum sizes, respectively. For 'Minimum' signal, set "0.13". In "Split" tab, set "2.60". In "Nuclei" tab, set "0.81". Select "use membrane signal to aid segmentation".
    3. Click "Segment cells" at the bottom part of the screen. Check the segmentation of nuclei and membranes of cells and retry with different parameters if it does not match the DAPI and membrane fluorescence of the cells.
    NOTE: The software recognizes the cells with the nuclear DAPI staining and based on the cell size. Adjust the cell parameters (size, split, pixels) according to the project.

6. Phenotype the cells.
    1. In the 'Phenotype' tab, click "add". Create cell phenotype categories: CD8 (blue dot)/CD8-PD-1 (red dot)/CD8-PD-1-Tim-3 (green dot)/other (black dot) (**Figure 4**).
    2. Select more than 5 examples of cells of each category. Click "Train classifier".
    NOTE: This generates a statistical classification algorithm by the software.
    3. Click "Phenotype all" to obtain the phenotype of each cell.
    NOTE: The software gives the phenotype of one cell with a confidence interval (CI) of accuracy.
    4. Improve the algorithm by training the software until the difference between eye and automated count is concordant (error < 5%). Choose a CI that is acceptable for the cells of interest.
    NOTE: We chose to make the training on the basis of 55% CI as acceptable.

7. Save the algorithm and project.
8. Under 'File' select "project". Name it and click "Save".

3. Perform batch analysis of the series.
    1. Select "Batch analysis". Select the project. Add the images to analyze. Select a folder of storage for the data. Click "Run". Check the quality of the composite image. Verify the phenotyping for all the images of the series.
    NOTE: The coupled image analysis software integrates all the cell compartments (membrane/cytoplasm/nuclei) signals. The phenotyping step is crucial albeit the training of the algorithm can be a time-consuming step. All the data of each image are in one .txt file. All the data of one cell (particularly its phenotype given with its CI) are in one line. For each slide, the image acquisition and subsequent counts were performed on 5 fields.

3. **Integration of the raw data and generation of the automated cell count**
    1. Compute the data with a statistical program.
        1. Compute all the data from the 5 images corresponding to the 5 fields analyzed for 1 patient. Use a statistical platform, and have an experienced statistician, data manager, or data scientist perform the analysis. Build a script that automatically counts the cells depending on their phenotype, selecting the CI > 55%.
        2. Put all the .txt files of the series in the same folder.

    2. Extract the data.
        1. Put all the .txt files in one folder. Run the automatic script built in step 3.3.1. Open the output .csv file generated by the R script. Save as .xl format. The output gathers the number of cells for each phenotype (*i.e.*, CD8 alone, CD8-PD-1, CD8-PD-1-Tim-3) for each patient.
        2. Calculate the average number of cells for each patient per field: divide the number of cells per the number of fields (*i.e.*, 5) to normalize the number of cells for each patient per field.
        3. Calculate the percentage of PD-1$^+$ cells among total CD8$^+$ T cells, and PD-1$^+$ Tim-3$^+$ cells among total CD8$^+$ T cells. See **Figure 5** for summary of this step.
        NOTE: R language (or other programming software of choice) is required to correctly create and execute the commands, and so an experienced user or statistician/data scientist is essential. The R program can compute the data of the same patient, but the name of the 5 .txt files of one patient should have an identical beginning, corresponding to a unique patient identifier.

4. **Statistical analysis**
    1. Use statistical software for the statistical analysis of the results.
    2. Perform appropriate statistical analyses with the help of a statistician.
        1. Use the non-parametric Wilcoxon's signed rank tests for comparison of PD-1 MFI between two cell phenotypes (**Figure 6**). Correlate the covariate and histological characteristics with a Pearson's chi-squared test.

2. Use a Kaplan-Meier method to estimate the progression free survival, and Cox regression models to estimate the covariate effects on time-to-event outcomes, such as overall survival and disease-free survival.
3. Consider *p*-values lower than 0.05 as significant.

Representative Results

Using the general protocol described above, we aimed to quantify intratumoral $CD8^+$ T cells co-expressing the inhibitory receptors PD-1 and Tim-3 in frozen tissues from patients with RCC, and to correlate the results with clinical outcomes[25].

Optimization of the CD8/PD-1/Tim-3 Staining:

Different species of antibodies (mouse, rabbit and goat, see **Table of Material**) were chosen in order to avoid cross reaction between the different antibodies. The protocol was validated on a tonsil, which is an organized lymphoid tissue. PD-1 staining could be found in the germinal centers (**Figure 1**), whereas CD8 and Tim-3 staining are present surrounding the germinal centers. The observation of this typical staining validated this protocol. The staining was also validated on the tissue of interest (kidney).

The absence of signal of the primary antibody incubated with their non-corresponding secondary antibody (data not shown) was confirmed. To analyze accurately the fluorescence staining and to make specific spectral libraries, individual slides were singly stained with each marker (CD8, PD-1, Tim-3, or DAPI) in the tissue of interest (kidney). A non-stained slide in the same conditions is necessary to extrapolate the autofluorescence of the tissue. The staining was analyzed by the automated microscope, which integrated the spectrums of the different fluorophores; each marker was well-differentiated and no overlap of markers was observed (**Figure 3**).

Quantitative and Qualitative Characteristics of the $CD8^+$ Infiltrate in 87 RCC Patients:

Results showed that approximatively half of $CD8^+$ T cells express PD-1 (mean 53.9%; SE: 30.49%) and about one third were double positive $PD\text{-}1^+$ $Tim\text{-}3^+$ (mean 38.16%; SE: 28.11%). Tim-3 expression without PD-1 expression was detected in less than 3% of $CD8^+$ T cells (data not shown). The mean numbers of $CD8^+$ T cell subpopulations were: total $CD8^+$ T cells 116.5 (SE: 216), $PD\text{-}1^+$ $CD8^+$T cells 89.32 (SE: 191.8), $PD\text{-}1^+$ $Tim\text{-}3^+$ 66.9 (SE: 143), and $PD\text{-}1^+$ $Tim\text{-}3^-$ $CD8^+$ T cells 22.38 (SE: 57.5) per field. The total number of intratumoral $CD8^+$ T cells was positively correlated with the percentage of $PD\text{-}1^+$ $Tim\text{-}3^+$ on $CD8^+$ T cells.

Functional Characterization of the $CD8^+$ T Cells Depending on Their Phenotype PD-1 and Tim-3:

PD-1 expression level is known to be correlated with T cell exhaustion so we next aimed to measure PD-1 expression on $CD8^+$ T cells according to Tim-3 expression status. As the mean fluorescence intensity of the different fluorochromes is reported at the cellular level, a small series of patients were manually analyzed for the cellular data: results showed a correlation of PD-1 membrane MFI with the cell subtype. PD-1 fluorescent intensity was measured (**Figure 6**) at the cellular level on $PD\text{-}1^+$ $Tim\text{-}3^+$ versus $PD\text{-}1^+$ $Tim\text{-}3^-$ $CD8^+$ T cells (A panel) and at the individual patient level after integrating these various cell signals on a tissue section. In a series of 9 patients, a comparison with Wilcoxon paired test found that PD-1 MFI is higher when Tim-3 is co-expressed, reinforcing the functional relevance of Tim-3 expression (B panel).

Expression of PD-1 and Tim-3 Ligands at the Surface of the Tumor Cells from Multiple Co-staining:

As T cell exhaustion is mediated through receptor/ligand interaction, we assessed the expression of PD-1 and Tim-3 ligands (PD-L1 and Galectin-9 (Gal-9), respectively) on renal tumor cells identified by pan-Keratin staining. Positivity is defined as a cut-off of 10% of tumor cells expressing the marker: (i) 58 out of 87 patients (66%) were positive for PD-L1; (ii) all the 15 tumors analyzed were positive for Gal-9 (**Figure 7A, B**).

Clinical Impact of the Co-expression of $Tim\text{-}3^+$ $PD\text{-}1^+$ on $CD8^+$ T Cells:

Tumor Node Metastasis (TNM) scoring, Fuhrman grade, tumor size, and UISS score are histological characteristics (combined with clinical score for UISS) used to define the prognosis value of primary RCC. A positive correlation was observed between the number and/or percentage of tumor-infiltrating $CD8^+$ T cells expressing PD-1 and Tim-3 (but not expressing only PD-1 without Tim-3) with all these parameters (**Table 1**). In line with this more pejorative phenotype, RCC patients with $CD8^+$ T cells co-expressing PD-1 and Tim-3 above the median percentage (34.7) were more likely to relapse ($p = 0.046$; HR 2.9; 95% CI: 1.02-8.21). This correlation was not observed with the percentage of PD-1 on $CD8^+$ T cells independently of Tim-3 status (**Table 2**). A correlation was also demonstrated between the percentage of $CD8^+$ T cells co-expressing PD-1 and Tim-3 and the 36-month overall survival rate (data not shown). We also validated the triple immunostaining on tonsil paraffin tissues (**Figure 1**).

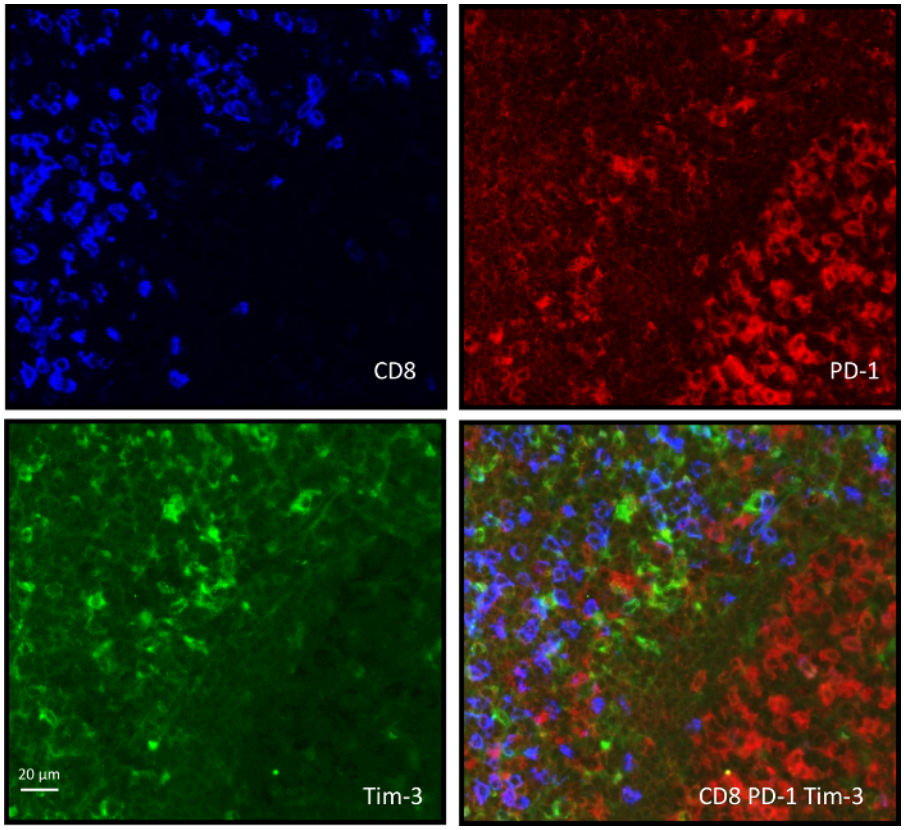

Figure 1: CD8-PD-1-Tim-3 immunostaining on a tonsil paraffin-embedded tissue. Paraffin embedded tissue sections instead of cryopreserved sections were selected for triple immunostaining. After dewaxing and rehydration, the same protocol of staining previously developed for cryopreserved sections was applied. $CD8^+$ T cells are located outside the germinal center and non-$CD8^+$ T cells expressing PD-1 are clustered in the germinal center. The microscope magnification is 20x and the scale bar represents 20 µm. Please click here to view a larger version of this figure.

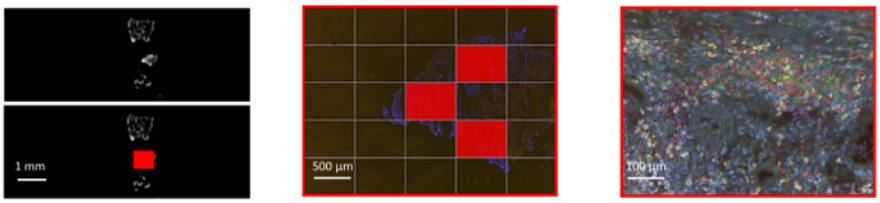

Figure 2: Automated analysis of renal cell carcinoma tissue specimens. After tissue recognition in bright field image (**A**, scale bar 1 mm), 4x microscope magnification low resolution imaging in RGB (red blue green conventional fluorescence) is used to select the fields (**B**, scale bar 500 µm. The full red square represents a field. A high-resolution image (multispectral cube fluorescence image specific to this technology) with at 20x magnification performed by the multispectral microscope is shown (**C**, scale bar 100 µm). Please click here to view a larger version of this figure.

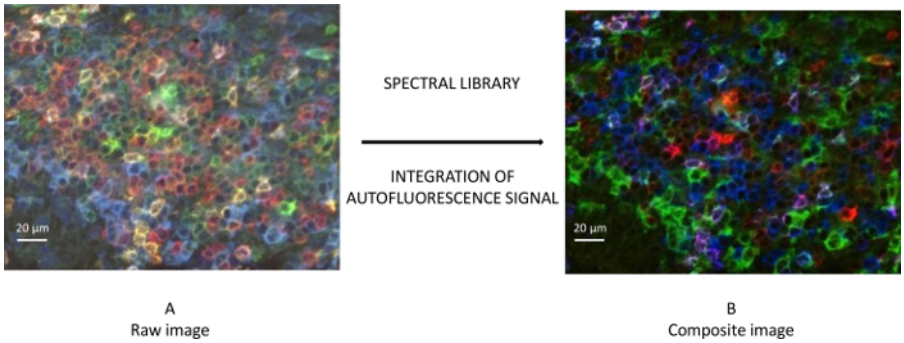

Figure 3: Multispectral microscopy and software coupled analysis for the generation of a composite image of a renal cell carcinoma (20x microscope magnification). The high resolution raw image (**A**) is a fluorescent image of the field after multispectral scanning by fluorescence filter cubes. Blue signal is AF488, Red is Cyanine 5, and green is Cyanin3. The merge shows different colors for example, yellow is a merge of the three fluorophores. This image is incorporated in the image analysis software. Spectral library integration allows an accurate spectrum separation of each fluorophore and autofluorescence leading to a fluorescent composite image (**B**). Representative colors are chosen by the operator: blue illustrates Cyanine 5 (CD8), Red Cyanine 3 (PD-1), Green AF488 (Tim-3). Merging mix color such as purple is used for CD8-PD-1 double positive. The scale bar represents 20 µm. Please click here to view a larger version of this figure.

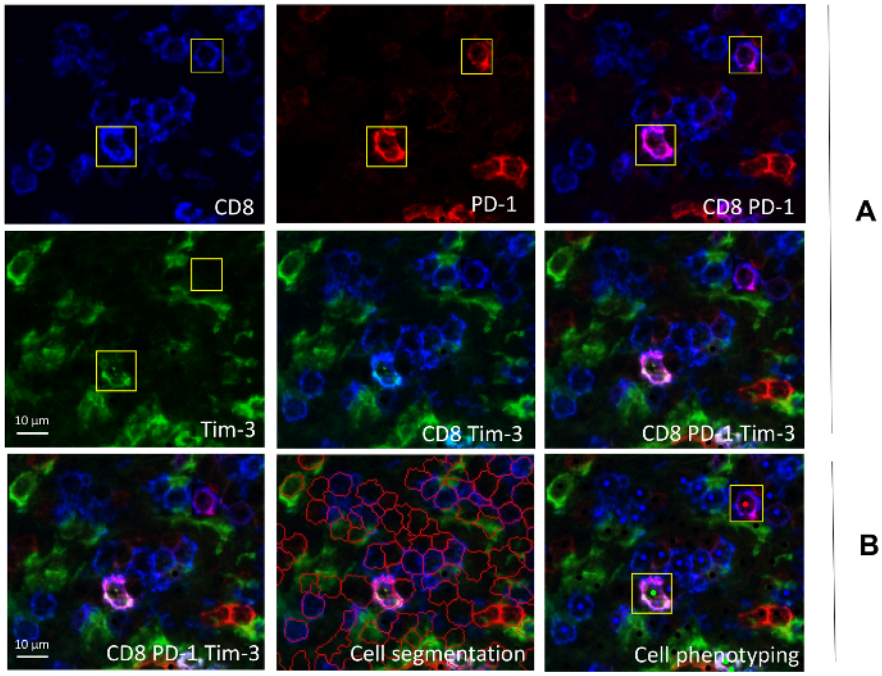

Figure 4: PD-1 and Tim-3 expression on tumor-infiltrating CD8$^+$ T cells on a clear cell renal cell carcinoma specimen analyzed by fluorescence multispectral imaging technology (20x microscope magnification). (**A**) CD8 (blue), PD-1 (red), and Tim-3 (green) were stained on frozen tissue sections derived from RCC patients. Colocalization of these three markers can be detected by merging the mono-staining pictures. Isotype controls were performed in each experiment. The scale bar represents 20 µm. Yellow boxes identify co-stained cells: a Tim-3$^-$ PD-1$^+$ CD8 cell and a Tim-3$^+$ PD-1$^+$ CD8 cell. (**B**) Triple co-staining for CD8, PD-1, and Tim-3 (merged) is shown on the left with the box indicating that green is CD8$^+$ T cells co-expressing PD-1 and/or Tim-3. For automated counting with the image analysis software, the identification of the cells relies on the presence of a nuclear staining (DAPI); the cell segmentation is also based on morphometric characteristics represented as red boundaries (middle panel). An algorithm trained by the user until concordance with visual count is performed (right), and after automated phenotyping, identifies green dots as CD8$^+$ T cells co-expressing PD-1 and Tim-3, red dots as CD8$^+$ T cells expressing PD-1 without Tim-3, and blue dots as CD8$^+$ T cells not expressing PD-1 or Tim-3. The scale bar represents 20 µm. Yellow box shows PD-1 and/or Tim-3 expressing CD8$^+$ T cells. Please click here to view a larger version of this figure.

Figure 5: Computing the raw data of multispectral analysis. Data of the count of each cell category present in each field (*i.e.*, 5 fields/patient, *i.e.*, 5 .txt files) are collected after image analysis. An R script combines the 5 fields data, only considering cells phenotyped with a confidence interval > 55%. The microscope magnification is 20x and the scale bar represents 100 µm. Please click here to view a larger version of this figure.

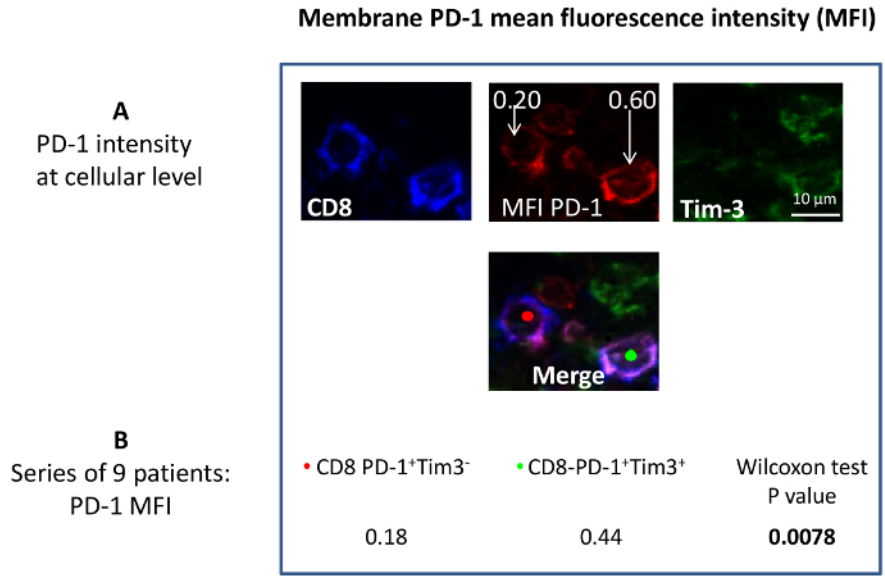

Figure 6: PD-1$^+$ Tim-3$^+$ CD8$^+$ T cells express higher levels of PD-1 compared to PD-1$^+$ Tim-3$^-$ CD8$^+$ T cells in renal cell carcinoma. The intensity of PD-1 is detected at the cellular level (left panel) by *in situ* immunofluorescence analysis on PD-1$^+$ Tim-3$^+$ and PD-1$^+$ Tim-3$^-$ CD8$^+$ T cells. At the individual level (middle panel): results are shown for the whole CD8$^+$ T cell subsets PD-1$^+$ Tim-3$^+$ versus PD-1$^+$ Tim-3$^-$ present on a tissue section (*i.e.*, one patient; Mann Whitney test). Comparative analysis of the mean PD-1 intensity was measured in a series of 9 patients (right panel) (Wilcoxon test, *p*-values lower than 0.05 were considered as significant). The microscope magnification is 20x and the scale bar represents 10 µm. Please click here to view a larger version of this figure.

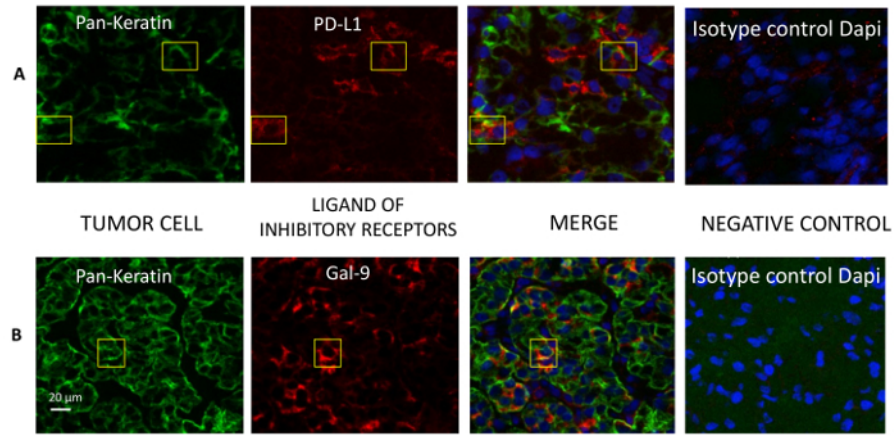

Figure 7: PD-L1 and Gal-9 *i.e.* PD-1 and Tim-3 ligands staining on renal cell carcinoma. (**A**) Tumor cells are identified by pan-Keratin staining. Co-staining of PD-L1 and pan-keratin (A panel) identifies the expression of PD-L1 on tumor cells in 58 patients out of 87 analyzed. (**B**) Galectin-9 was expressed in all of the 15 tumors from RCC patients analyzed. Positivity was considered if at least 10% of cells were stained for the marker analyzed. Isotype controls were included for each staining. Yellow boxes represent positive tumor (pan-Keratin+) cells for PD-L1 (panel A) or Galectin-9 (panel B). The microscope magnification is 20x and the scale bar represents 20 µm. Please click here to view a larger version of this figure.

%/CD8$^+$ T cells	PD-1$^+$	PD1$^+$ Tim-3$^+$	PD-1$^+$ Tim-3$^-$
TNM	**0.04**	**0.003**	0.22
Furhman	**0.01**	**0.004**	0.74
Tumor Size	0.08	**0.01**	0.37
UISS	**0.01**	**0.01**	0.63

Table 1: Correlation between the expression of PD-1 alone or combined with Tim-3 on CD8$^+$ T cells and clinical prognostic parameters of RCC patients: *p*-values. The percentage of PD-1$^+$, PD-1$^+$ Tim-3$^+$ or PD-1$^+$ Tim-3$^-$ on CD8$^+$ T cells selected as a continuous variable measured by *in situ* immunofluorescence in the cohort of 87 patients was correlated with various clinical parameters defined as a binary (TNM, Fuhrman grade, UISS score) or a continuous variable (tumor size). TNM was divided into two groups: localized disease (pT1 and pT2) and advanced disease (pT3, pT4, N$^+$, or M$^+$). Fuhrman grade was defined as low (grade I or II) and high (grade III or IV) and the UISS score was divided into 3 classes (0, 1, and 2). *P*-values indicating a significant correlation are shown in bold.

CD8$^+$ T cell subset/CD8	PD-1$^+$ Tim-3$^+$	PD-1$^+$ Tim-3$^-$
Median (%)	34.7	8.6
Correlation with PFS	**P = 0.046**	P = 0.8

Table 2: Correlation between PD-1 and Tim-3 co-expression on CD8$^+$ T cells and progression free survival. Two groups of RCC patients (n = 87) depending on the percentage of PD-1 without Tim-3 (right), PD-1 and Tim-3 (Left) relative to the median were individualized. The correlation with the PFS was made with the median selected as a cut-off. *P*-values indicating a significant correlation are shown in bold.

Supplemental Table 1: Buffer composition of TBS and TBST. TBS is used for antibody mixes and dilutions. For washes, all steps are performed with TBS except for the washes following primary antibodies, where TBST is recommended. Please click here to download this file.

Supplemental Table 2: Detailed antibodies mix composition for CD8-PD-1-Tim-3 immunofluorescence staining. For each primary, secondary, and tertiary antibody mixes, the dilution to perform in the corresponding volume of TBS is given for a total volume of 1 mL. For one slide, the necessary total reaction volume is 100 µL for a tissue area of 2 cm^2. Please click here to download this file.

Discussion

Modifications and Troubleshooting:

The tissue quality is an important parameter; it can be easily checked by hematoxylin and eosin coloration.

One advantage of the technique is the possibility of multiplexed stainings, but to avoid fluorophore spillover, it recommended to choose emission wavelengths with delta of 10 nm minimum. Here, because we had 4 stainings including DAPI, we chose to spread out the wavelengths (DAPI: 460 nm, AF488: 519 nm, Cyanine 3: 570 nm, Cyanine 5: 670 nm). The risk of overlapping signals from various fluorophores is avoided by using the software to compute the pure spectrum of a fluorophore from a mixed emission signal, combined with an automated image analysis. The mono-stained slides also confirm the absence of overlap between fluorophores and act as a compensation thanks to the spectral library.

Sometimes positivity for one marker in one cell can be difficult to determine if the staining/fluorescence is weak. The negative control included in each experiment is a good way to determine a threshold of positivity.

In the coupled software used to analyze images, a scoring step for determining the positivity of the cell exists but it only can analyze two markers simultaneously. Because we can have triple staining on the same cell (CD8, PD-1, and Tim-3), we chose the phenotyping step.

The phenotyping step can be laborious, particularly if the type of staining and background is variable from one sample to another.

Limitations of the Technique:

Even if the number of co-stainings is an advantage compared to conventional fluorescence, it is not possible to analyze many colors as in flow cytometry. Especially when the colocalization of multiple markers is studied, be aware for sensitivity that is lower compared with confocal microscopy (for a 20x microscope magnification, approximately 0.5 µm versus 0.1 µm per pixel for confocal, depending on the brand) and check for fluorophore spillover (refer to Critical Steps Within the Protocol, below).

A large limitation of the technique is the raw data format. The raw data are .txt files which might be tricky to use. As the software gives one .txt file per image with CI for the phenotype, the manual treatment of each of the 5 files per patient of a huge series is very laborious. A bioinformatics specialist is required to compute all the data in a statistical software.

Significance with Respect to Existing Methods:

Multiplexed staining analysis is easily possible. Compared to flow cytometry, which analyzes fresh samples, this technique allows a rapid counting in a reproducible method of the different cell subsets present in the tumor microenvironment, in large cohorts of frozen samples with an automated procedure[26,27]. We could automatically count infiltrating CD8$^+$ T cells expressing PD-1 and co-expressing Tim-3 or not in the setting of RCC. The automatic count avoids several biases like eye fatigue and non-reproducible count, and is not time consuming.

As the large cohort studied was on frozen sample, we had retrospective data so we could link the absolute number or percentage of the $CD8^+$ T cell subsets with biological parameters and clinical outcome. As there is an important heterogeneity of the immune infiltration from one patient to another[28], this represents an advantage compared to fluorocytometry that reports only MFI and percentage but not the infiltration grade.

The fluorescence intensity is quantitatively reported for each cell, and in the different cell compartments (membrane/cytoplasm/nuclei), we could evaluate the level of PD-1 staining by MFI at the membrane. This represents another interesting tool that is similar to flow cytometry. We found that the $PD\text{-}1^+$ $CD8^+$ T cells expressing Tim-3 had higher expression of PD-1 and were associated with a poor prognosis (impact on progression free survival). To our knowledge, it is the first study using this method that shows a clinical significance of a specific cell subset.

Future Applications:

The field of application is immense. We also highlighted in lung cancer tumor's microenvironment another specific cell subset: the tissue resident memory T cells called TRM ($CD103^+$ $CD49a^+$), and they are correlated with a better overall survival[21,29,30]. In another work using this technique, our team found that PD-L1 was overexpressed on tumor cells in a subtype of lung cancer with an anaplastic lymphoma kinase (ALK) rearrangement, and this expression was correlated with $CD8^+$ T infiltrate[10]. This technique is suitable for the evaluation of critical biological parameters in several contexts and can represent a valuable tool for biomarker discovery. Since the xy coordinates are given, it is one of the first tools to study the topography and cell/cell interactions with ease[31].

Critical Steps Within the Protocol:

One of the critical steps is the optimization of the co-staining, which can be time-consuming. The choice of a good antibody is crucial, for instance multiple clones have been tested for Tim-3 in the present case. Furthermore, different fluorophores for the same marker can give different results so it is important to try several combinations. Examining the staining specificity with antibodies that should not react together is recommended. Despite the possibility to analyze several fluorophores at the same time, checking for spillover with the mono-stained slides is recommended. Another crucial step is the phenotyping step that relies on manual training to perform carefully.

In total, the use of this multiplexed technique by an adept operator represents an elegant tool to analyze multiple cell subsets of the local immune infiltrate, which is of importance since the peripheral blood analysis cannot be representative of the local tumor environment.

Disclosures

All authors have no conflict of interest to declare.

Acknowledgements

This work was supported by grants from Institut National du Cancer (INCA) (ET), Ligue contre le Cancer (ET), Université Sorbonne Paris Cité (ET), ANR (Selectimmunco) (ET), Labex Immuno-Oncology (ET), SIRIC CARPEM (CG, ET). EdG was funded by a fellowship of Fondation ARC. EV and CD were funded by a fellowship of APHP (bourse année recherche). ChB is funded by a fellowship of Université Sorbonne Paris Cité (contrat doctoral). The authors thank Bristol Myers Squibb for their funding in this project. The authors thank the department of Pathology of Hopital Européen Georges Pompidou and Necker (Laurianne Chambolle, Elodie Michel and Gisèle Legall). The authors thank the Histology platform of PARCC, Hopital Européen Georges Pompidou (Corinne Lesaffre).

References

1. Borghaei, H. *et al.* Nivolumab versus Docetaxel in Advanced Nonsquamous Non-Small-Cell Lung Cancer. *N Engl J Med.* **373** (17), 1627-1639 (2015).
2. Granier, C. *et al.* [Cancer immunotherapy: Rational and recent breakthroughs]. *Rev Med Interne.* **37** (10), 694-700 (2016).
3. Motzer, R. J. *et al.* Nivolumab for Metastatic Renal Cell Carcinoma: Results of a Randomized Phase II Trial. *J Clin Oncol.* **33** (13), 1430-1437 (2015).
4. Robert, C. *et al.* Nivolumab in previously untreated melanoma without BRAF mutation. *N Engl J Med.* **372** (4), 320-330 (2015).
5. Robert, C. *et al.* Ipilimumab plus dacarbazine for previously untreated metastatic melanoma. *N Engl J Med.* **364** (26), 2517-2526 (2011).
6. Rosenberg, J. E. *et al.* Atezolizumab in patients with locally advanced and metastatic urothelial carcinoma who have progressed following treatment with platinum-based chemotherapy: a single-arm, multicentre, phase 2 trial. *Lancet.* **387** (10031), 1909-1920 (2016).
7. Schadendorf, D. *et al.* Pooled Analysis of Long-Term Survival Data From Phase II and Phase III Trials of Ipilimumab in Unresectable or Metastatic Melanoma. *J Clin Oncol.* **33** (17), 1889-1894 (2015).
8. Ribas, A., & Hu-Lieskovan, S. What does PD-L1 positive or negative mean? *J Exp Med.* **213** (13), 2835-2840 (2016).
9. Rizvi, N. A. *et al.* Cancer immunology. Mutational landscape determines sensitivity to PD-1 blockade in non-small cell lung cancer. *Science.* **348** (6230), 124-128 (2015).
10. Roussel, H. *et al.* Composite biomarkers defined by multiparametric immunofluorescence analysis identify ALK-positive adenocarcinoma as a potential target for immunotherapy. *OncoImmunology.* **6** (4), e1286437 (2017).
11. Pages, F., Granier, C., Kirilovsky, A., Elsissy, C., & Tartour, E. *Bull Cancer.* **103 Suppl 1** S151-S159 (2016).
12. Tumeh, P. C. *et al.* PD-1 blockade induces responses by inhibiting adaptive immune resistance. *Nature.* **515** (7528), 568-571 (2014).
13. Fourcade, J. *et al.* Upregulation of Tim-3 and PD-1 expression is associated with tumor antigen-specific CD8+ T cell dysfunction in melanoma patients. *J Exp Med.* **207** (10), 2175-2186 (2010).
14. Koyama, S. *et al.* Adaptive resistance to therapeutic PD-1 blockade is associated with upregulation of alternative immune checkpoints. *Nat Commun.* **7** 10501 (2016).
15. Wherry, E. J., & Kurachi, M. Molecular and cellular insights into T cell exhaustion. *Nat Rev Immunol.* **15** (8), 486-499 (2015).
16. Cai, C. *et al.* Tim-3 expression represents dysfunctional tumor infiltrating T cells in renal cell carcinoma. *World J Urol.* **34** (4), 561-567 (2016).

17. Sakuishi, K. *et al.* Targeting Tim-3 and PD-1 pathways to reverse T cell exhaustion and restore anti-tumor immunity. *J Exp Med.* **207** (10), 2187-2194 (2010).
18. Stack, E. C., Wang, C., Roman, K. A., & Hoyt, C. C. Multiplexed immunohistochemistry, imaging, and quantitation: a review, with an assessment of Tyramide signal amplification, multispectral imaging and multiplex analysis. *Methods.* **70** (1), 46-58 (2014).
19. Bethmann, D., Feng, Z., & Fox, B. A. Immunoprofiling as a predictor of patient's response to cancer therapy-promises and challenges. *Curr Opin Immunol.* **45** 60-72 (2017).
20. Badoual, C. *et al.* PD-1-expressing tumor-infiltrating T cells are a favorable prognostic biomarker in HPV-associated head and neck cancer. *Cancer Res.* **73** (1), 128-138 (2013).
21. Nizard, M. *et al.* Resident memory T cells plays a key role in the efficacy of cancer vaccine. *Nat Commun.* **8** 15221 (2017).
22. Nghiem, P. T. *et al.* PD-1 Blockade with Pembrolizumab in Advanced Merkel-Cell Carcinoma. *N Engl J Med.* **374** (26), 2542-2552 (2016).
23. Roussel, H. *et al.* Composite biomarkers defined by multiparametric immunofluorescence analysis identify ALK-positive adenocarcinoma as a potential target for immunotherapy. *Oncoimmunology.* (4), (2017).
24. Woods, K. *et al.* Mismatch in epitope specificities between IFNgamma inflamed and uninflamed conditions leads to escape from T lymphocyte killing in melanoma. *J Immunother Cancer.* **4** 10 (2016).
25. Granier, C. *et al.* Tim-3 Expression on Tumor-Infiltrating PD-1+CD8+ T Cells Correlates with Poor Clinical Outcome in Renal Cell Carcinoma. *Cancer Res.* **77** (5), 1075-1082 (2017).
26. Feng, Z. *et al.* Multispectral Imaging of T and B Cells in Murine Spleen and Tumor. *J Immunol.* **196** (9), 3943-3950 (2016).
27. Feng, Z. *et al.* Multispectral imaging of formalin-fixed tissue predicts ability to generate tumor-infiltrating lymphocytes from melanoma. *J Immunother Cancer.* **3** 47 (2015).
28. Fridman, W. H., Pages, F., Sautes-Fridman, C., & Galon, J. The immune contexture in human tumours: impact on clinical outcome. *Nat Rev Cancer.* **12** (4), 298-306 (2012).
29. Nizard, M., Roussel, H., & Tartour, E. Resident Memory T Cells as Surrogate Markers of the Efficacy of Cancer Vaccines. *Clin Cancer Res.* **22** (3), 530-532 (2016).
30. Sandoval, F. *et al.* Mucosal imprinting of vaccine-induced CD8(+) T cells is crucial to inhibit the growth of mucosal tumors. *Sci Transl Med.* **5** (172), 172ra120 (2013).
31. Carstens, J. L. *et al.* Spatial computation of intratumoral T cells correlates with survival of patients with pancreatic cancer. *Nat Commun.* **8** 15095 (2017).

